A New Technique for the Examination of Tracheal Tumors

The Bronchoscopic Turned Around Procedure

Shinichi Yamamoto, MD, Tetsuya Endo, MD, Kenji Tetsuka, MD, PhD, and Shunsuke Endo, MD, PhD

Reprinted from *J Bronchol Intervent Pulmonol* • Volume 17, Number 3, July 2010

A New Technique for the Examination of Tracheal Tumors

The Bronchoscopic Turned Around Procedure

Shinichi Yamamoto, MD, Tetsuya Endo, MD, Kenji Tetsuka, MD, PhD, and Shunsuke Endo, MD, PhD

Abstract: Flexible bronchoscopy is useful for confirming an endotracheal tumor. However, observation of the distal end of the tumor is difficult because of the presence of the lesion itself. Here we describe a technique that we termed "bronchoscopic turned around procedure," which can be used to observe the distal extent of the lesion using an ultrathin bronchoscope. The scope is passed distal to the endotracheal tumor and is flexed upward by 180 degrees in the trachea for full visualization of the distal extent of the lesion and the airway anatomy. We found this procedure to be an effective technique to assess surgical candidates by confirming the surface structure of the tracheal lumen, which cannot be obtained by computed tomography or virtual bronchoscopy.

Key Words: electrocautery, tracheal tumor, ultrathin bronchoscopy

(*J Bronchol Intervent Pulmonol* 2010;17:273–275)

Flexible bronchoscopy is a useful technique for observing tracheal tumors. However, observation of the distal edge of the tumor is difficult because of a blind spot caused by polypoid tumors. We describe the "bronchoscopic turned around procedure," which overcomes this limitation by inserting an ultrathin bronchoscope on the distal end of the tracheal tumor and flexing the bronchoscope upward by 180 degrees.

METHODS

We used an ultrathin bronchoscope (BF-XP260F; Olympus, Tokyo, Japan) to observe the distal end of the tracheal tumor. In accordance with computed tomography before the bronchoscopy, we measured the internal diameter of the distal end of the tumor. The diameter of the area occupied by the ultrathin bronchoscope that was flexed upward by 180 degrees was 13 mm. If the internal diameter of the distal end of the tumor exceeded 13 mm, then the bronchoscopic turned around procedure was considered to be possible.

Under general anesthesia with endotracheal intubation, an ultrathin bronchoscope was inserted beyond the distal end of the tumor through the obstruction caused by the tumor, and the bronchoscope was flexed upward by 180 degrees at the carina to form a "J" shape. The bronchoscope was then pulled up to the distal end of the tumor while keeping its "J" configuration. We named this technique the "bronchoscopic turned around procedure" (Fig. 1). After observation, the ultrathin bronchoscope was straightened and removed.

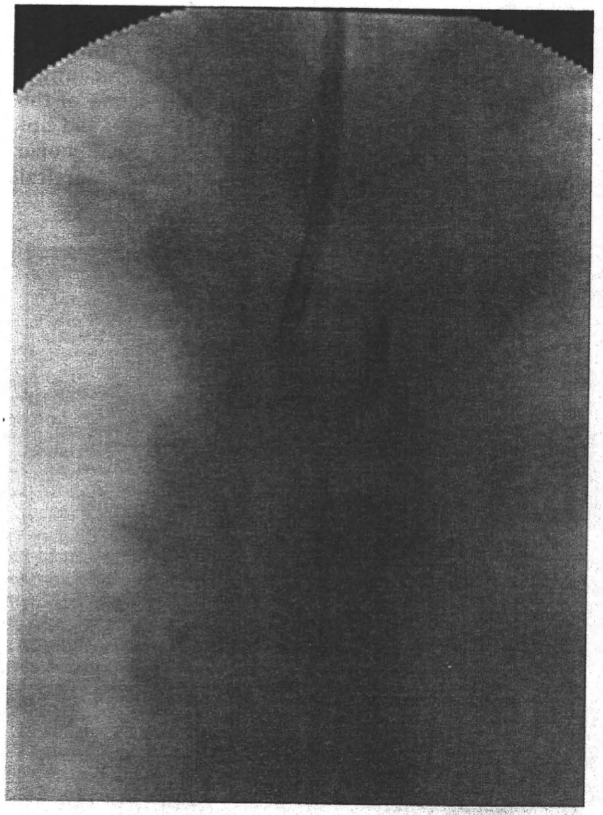

FIGURE 1. The "bronchoscopic turned around procedure." An ultrathin bronchoscope is flexed upward by 180 degrees to observe the distal end of a tracheal tumor.

Received for publication March 31, 2010; accepted June 1, 2010.
From the Division of General Thoracic Surgery, Department of Surgery, Jichi Medical University, Tochigi, Japan.
There is no conflict of interest.
Reprints: Shinichi Yamamoto, MD, Division of General Thoracic Surgery, Department of Surgery, Jichi Medical University, 3311-1, Yakushiji, Shimotsuke, Tochigi 329-0498, Japan (e-mail: tcvyamap@jichi.ac.jp).

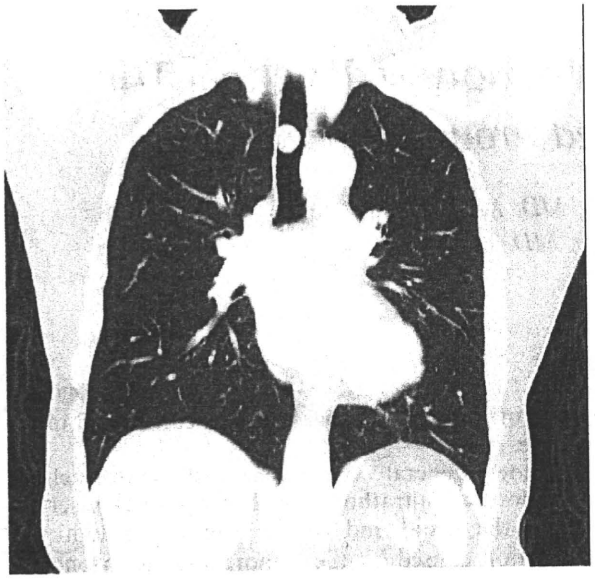

FIGURE 2. Computed tomography showed a tracheal tumor, which almost completely occluded the trachea.

CASE REPORT

A 66-year-old woman was admitted for cough and stridor. Computed tomography showed a tracheal tumor, with the longest diameter of approximately 10 mm and the inner tracheal diameter of the distal end of the tumor of 16 mm (Fig. 2). The distal end of the tumor was difficult to observe because it was difficult to safely insert a conventional bronchoscope (Fig. 3) and the trachea behind the tumor was in a blind spot. Using the bronchoscopic turned around procedure, we accurately gauged the extent of the lesion and found that the distal end of the tumor did not infiltrate the surrounding tissue (Fig. 4). The bronchoscopic findings clearly suggested that the patient was a surgical candidate for tracheal sleeve resection. Bronchoscopic tumor resection with electrocautery and argon plasma coagulation enabled endotracheal intubation and was followed by a tracheal sleeve resection of 5 tracheal rings. The bronchoscopy and tracheal reconstruction were uneventful.

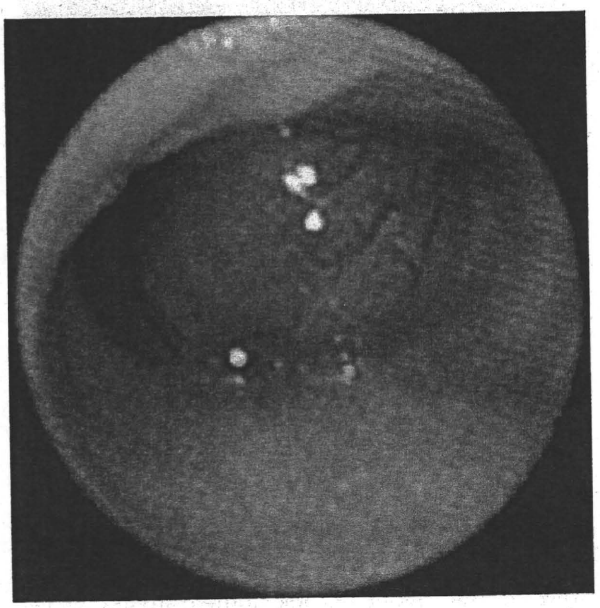

FIGURE 3. Bronchoscopic findings: Flexible bronchoscopy showed a tracheal tumor with a diameter of 1 cm.

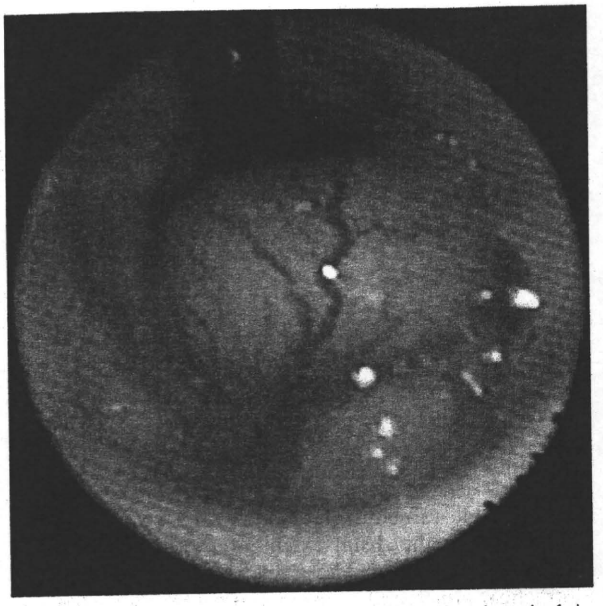

FIGURE 4. Bronchoscopic findings of the distal end of the tumor. Ultrathin bronchoscopy showed the distal end of the tumor and the ultrathin bronchoscope itself.

DISCUSSION

An ultrathin bronchoscope is used for the diagnosis of peripheral lung lesions and the assessment of central airway obstruction.[1] An ultrathin bronchoscope is incidentally retroflexed[2] after its insertion into the upper bronchus. By exploiting this retroflexion, the bronchoscopic procedure can identify the distal end of tracheal tumors, which cannot be observed by conventional bronchoscopic procedures.

Virtual bronchoscopy is also useful for the observation of regions that cannot be visualized by conventional bronchoscopy.[3–5] However, virtual bronchoscopy cannot be used to view the surface structure of the tracheal lumen in detail. The bronchoscopic turned around procedure can provide a more detailed observation of mucosal lesions, such as tumors, in the distal end of the trachea.

The bronchoscopic turned around procedure could result in complications, as repeated bending at 180 degrees of the ultrathin bronchoscope may lead to bronchial injury and damage to the fiber optic bundle.[6–8] Prakash reported "turnaround of flexible bronchoscopy" as a complication of the procedure, which damaged the fibers and angulation wires and caused significant respiratory compromise to the patient.[8] Before the procedure, we confirmed that the diameter of the trachea, as measured by

computed tomography,[9] was larger than the ultrathin bronchoscope when retroflexed upward by 180 degrees. Thus, we were convinced that the bronchoscopic turned around procedure would be possible without contact between the ultrathin bronchoscope and the bronchial wall. We can avoid these complications by measuring the internal diameter of the trachea using computed tomography and by confirming that the bronchoscope is not damaged before the procedure.

ACKNOWLEDGMENT

The authors thank Dr H. Takahashi (Department of General Thoracic Surgery, Shuwa General Hospital, Saitama, Japan) for his valuable comments and assistance with this technique.

REFERENCES

1. Schuurmans MM, Michaud GC, Diacon AH, et al. Use of an ultrathin bronchoscope in the assessment of central airway obstruction. *Chest*. 2003;124:735–739.
2. Mueller DK, Foiles SR. Right mainstem bronchial kink after right upper lobectomy. *Ann Thorac Surg*. 2007;84:1401.
3. Mark Z, Bajzik G, Nagy A, et al. Comparison of virtual and fiberoptic bronchoscopy in the management of airway stenosis. *Pathol Oncol Res*. 2008;14:313–319.
4. Bauer TL, Steiner KV. Virtual bronchoscopy: clinical applications and limitations. *Surg Oncol Clin N Am*. 2007; 16:323–328.
5. Shitrit D, Valdsislav P, Grubstein A, et al. Accuracy of virtual bronchoscopy for grading tracheobronchial stenosis: correlation with pulmonary function test and fiberoptic bronchoscopy. *Chest*. 2005;128:3545–3550.
6. Schneider T, Storz K, Dienemann H, et al. Management of iatrogenic tracheobronchial injuries: a retrospective analysis of 29 cases. *Ann Thorac Surg*. 2007;83:1960–1964.
7. Hari CK, Petheram T, Garth R. Unusual complication of reusable suction catheter during rigid bronchoscopy. *Eur Arch Otorhinolaryngol*. 2007;264:1509–1511.
8. Prakash UB, ed. *Bronchoscopy*. 1st ed. New York: Raven Press Ltd; 1994.
9. Olivier P, Hayon-Sonsino D, Convard JP, et al. Measurement of left mainstem bronchus using multiplane CT reconstructions and relationship between patient characteristics or tracheal diameters and left bronchial diameters. *Chest*. 2006;130:101–107.

Thymic clear cell carcinoma

Tomoyuki Nakano, MD · Shunsuke Endo, MD · Hiroyoshi Tsubochi, MD
Mitsuhiro Nokubi, MD · Yasutaka Watanabe, MD · Shinichiro Koyama, MD

Department of General Thoracic Surgery and Pulmonary Medicine, Jichi Medical University and Saitama Medical Center, Tochigi, Japan

General Thoracic and Cardiovascular Surgery
Official Publication of
The Japanese Association for Thoracic Surgery

Vol. 58 No. 2, pp. 98-100, February, 2010

Gen Thorac Cardiovasc Surg (2010) 58:98–100
DOI 10.1007/s11748-009-0481-6

CASE REPORT

Thymic clear cell carcinoma

Tomoyuki Nakano, MD · Shunsuke Endo, MD
Hiroyoshi Tsubochi, MD · Mitsuhiro Nokubi, MD
Yasutaka Watanabe, MD · Shinichiro Koyama, MD

Received: 20 January 2009 / Accepted: 18 May 2009

Abstract We report a 42-year-old man with a rare thymic clear cell carcinoma. Marked nodal metastases involved right hilar, mediastinal, and left supraclavicular regions. Complete resection including thymothymectomy, cervicomediastinal nodal dissection, and right upper lobectomy with hilar lymphadenectomy was successful. Postoperative chemoradiation therapy was uneventful. The patient had no recurrence or metastasis until brain metastasis occurred 1 year after surgery.

Key words Thymic cancer · Clear cell carcinoma · Lymphatic metastasis · Surgery · Multimodal treatment

Introduction

Thymic cancer occurs less frequently than thymic epithelial cancer and has a wide variety of histological types. High-grade malignant thymic carcinoma shows an invasive pattern with or without nodal involvement. Some reports describing the efficacy of combined modes of therapy have been presented. A treatment guideline for thymic cancer has not yet been proposed. We herein describe trimodal treatment for a rare high-grade clear cell carcinoma involving massive metastasis to the cervicomediastinal lymph nodes.

T. Nakano · S. Endo (✉) · H. Tsubochi · M. Nokubi · Y. Watanabe · S. Koyama
Department of General Thoracic Surgery and Pulmonary Medicine, Jichi Medical University and Saitama Medical Center, 1-3311 Yakushiji, Shimotsuke, Tochigi 329-0498, Japan
Tel. +81-285-58-7368; Fax +81-285-44-6271
e-mail: tcvshun@jichi.ac.jp

Case

A 42-year-old man presented to our hospital for investigation of an asymptomatic mediastinal tumor. Blood tests showed that the serum C-reactive protein (CRP) level was slightly increased to 0.99 mg/dl, and serum concentrations of carcinoembryonic antigen (CEA) and squamous cell carcinoma-related antigen were elevated to 9.2 ng/ml and 3.4 ng/ml, respectively. Chest radiography revealed enlargement of an upper mediastinal shadow.

Computed tomography (CT) revealed an anterior mediastinal tumor at the left side of the ascending aorta that was 30 mm in diameter with a homogeneous component (Fig. 1A). Marked lymphadenopathy was apparent at the right upper mediastinum and the hilum of the right upper lobe. There were no abnormal findings of intraabdominal organs and no lymphadenopathy in other regions. Positron emission tomography (PET) revealed fluorodeoxyglucose uptake at the tumor, the enlarged lymph nodes found on the CT scan, and the left supraclavicular lymph nodes (Fig. 1B). Bronchoscopy did not reveal any abnormal findings in the bronchial lumen. No cervical lymph nodes were palpable.

Incisional biopsy for an anterior mediastinal tumor via left-sided thoracoscopy led to the diagnosis of epithelial cancer. The intraoperative diagnosis based on the histological study and PET findings was thymic epithelial cancer.

Complete resection via median sternotomy and cervical incision in the supine position was performed. Lymph nodes located at the right upper mediastinum, the hilum of the right upper lobe, and at the left supraclavicular lesions were resected (Fig. 2). A concomitant right upper lobectomy was necessary because hilar lymph nodal

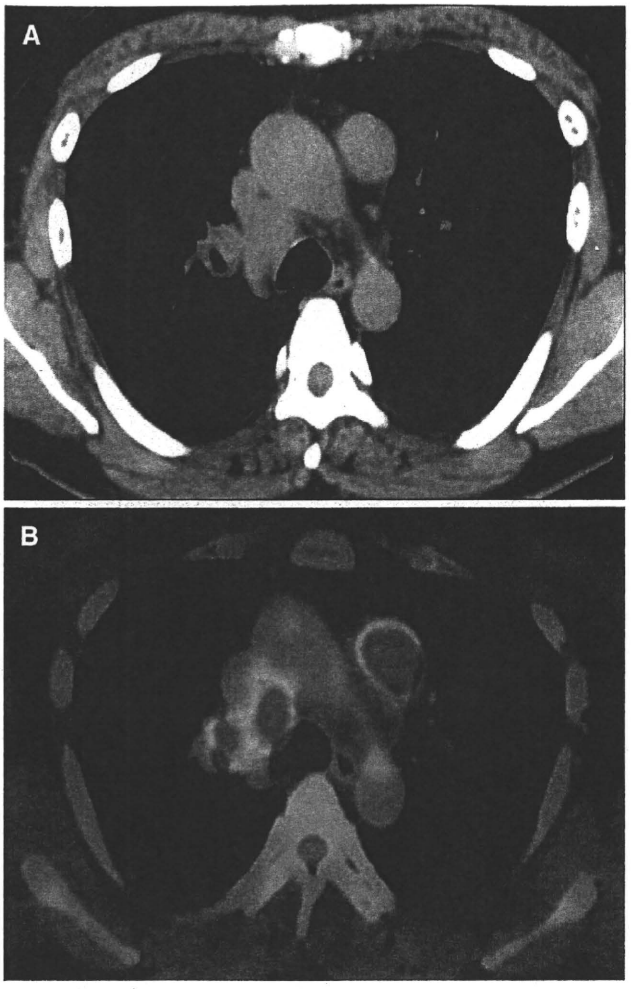

Fig. 1 **A** Computed tomography (CT) shows an anterior mediastinal tumor located at the left side of the ascending aorta and enlarged lymph nodes at the right upper mediastinum and the hilum of the right upper lobe. **B** Positron emission tomography reveals fluorodeoxyglucose uptake at the tumor and the enlarged lymph nodes found on the CT scans

involvement in the right upper lobe was marked. Pathological findings (Fig. 3A) revealed a clear cell carcinoma. Immunohistochemical studies were positive for keratin, slightly positive for CD5, and CEA staining was focally positive (Fig. 3B). Thyroid transcription factor-1, vimentin, placental alkaline phosphatase, leukocyte common antigen, and protein S-100B were negative. The pathological diagnosis was a clear cell carcinoma type of thymic cancer.

The patient was discharged on postoperative day 14. Serum CEA concentration decreased to 1.7 ng/ml. The patient received the following concurrent chemoradiation therapy: four cycles of chemotherapy of adriamycin, cyclophosphamide, vincristine, and cisplatin; irradiation of a total 50 Gy to mediastinal and left supraclavicular regions. The patient had no recurrence or

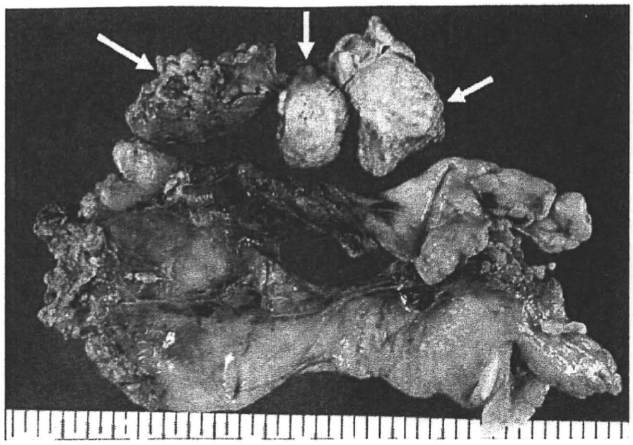

Fig. 2 Macroscopic findings show the primary tumor, which was divided (*arrows*), and the additionally resected thymus via median sternotomy

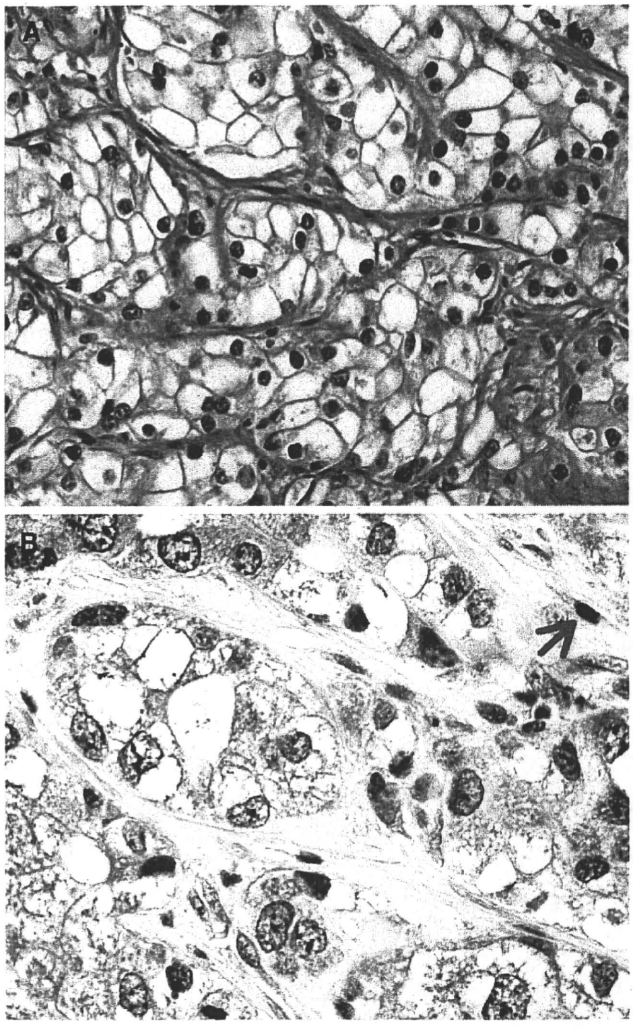

Fig. 3 **A** Hematoxylin-eosin staining reveals a clear cell carcinoma. Note the nests and cords of tumor cells with optically lucent cytoplasm. **B** Immunohistochemical study of CD5 staining revealed that nested tumor cells were weakly positive for CD5. *Arrow* indicates a CD5+ T lymphocyte (positive control)

metastasis until brain metastasis occurred 1 year after surgery.

Discussion

Thymic cancer had been previously treated as a subtype of malignant thymoma because of its rarity. In 1978, Levine and Rosai defined it as a disease biologically distinct from malignant thymoma in terms of nuclear immunohistochemistry.[1] Two groups and eight types were stratified by histological variation based on the tumors' oncological behavior according to the Suster and Rosai classification.[2] The low-grade malignancy group includes well-differentiated squamous cell carcinoma, mucoepidermoid carcinoma, and basaloid carcinoma. The high-grade malignancy group includes lymphoepithelioma-like carcinoma, small cell/neuroendocrine carcinoma, clear cell carcinoma, sarcomatoid carcinoma, and undifferentiated/anaplastic carcinoma. Clear cell carcinomas have been described in a variety of organs, most commonly in the kidney, ovary, and lung but also in the pancreas[3] and thyroid.[4] Metastasis from renal clear cell carcinoma or ovarian clear cell carcinoma should be excluded in patients with thymic clear cell carcinoma. The cells usually express epithelial membrane antigen and have a rather bland appearance and low mitotic count in contrast to their aggressive clinical behavior. The clear cell phenotype represents a secondary change superimposed on typical thymic cancer,[5] whereas in the latest World Health Organization (WHO) scheme clear cell carcinoma is considered to be a distinct subtype.

According to the report of eight cases of thymic clear cell carcinoma by Hasserjian et al.,[5] the median survival from diagnosis among the patients who died of disease was 13 months (range 4 months to 2 years). Clear cell carcinoma is difficult to diagnose because of ill-defined symptoms, and it is often discovery incidentally. Delay to diagnosis may contribute to the large tumor size attained by the time of resection and to the high incidence of incomplete resections. Patients who underwent incomplete resection had a poorer prognosis than those who underwent complete resection.

Treatment for thymic cancer remains to be established. Complete resection is the best way to a cure but is often impossible. Therefore, in our patient complete resection concomitant with right upper lobectomy was performed to obtain the diagnosis of thymic epithelial cancer. A surgical procedure, especially if not radical, may be complemented by radiotherapy.[6] Preoperative chemotherapy has been recommended to reduce the volume of a tumor to allow complete resection and to increase the survival rate.[7] The benefits of postoperative chemotherapy are unclear.[8] A multimodal therapeutic approach requires further investigations with multicenter studies. In addition, thymic clear cell carcinoma is rare, so treatment protocols have not been established. Clear cell carcinoma also occurs in other organs such as kidneys and ovaries. These cases are resistant to conventional cytotoxic agents. New biological agents for thymic cancer should be investigated, such as vascular endothelial growth factor (VEGF) receptor inhibitors (sunitinib and sorafenib), an anti-VEGF antibody (bevacizumab), and a mammalian target of rapamycin inhibitor used for renal clear cell carcinoma.[9]

Conclusion

We report a patient with a rare, aggressive thymic clear cell carcinoma. Despite trimodal treatment, brain metastasis occurred 1 year after surgery in our patient. Development of new pharmaceutical agents effective against clear cell carcinoma is desirable.

References

1. Levine GD, Rosai J. Thymic hyperplasia and neoplasia: a review of current concepts. Hum Pathol 1978;9;495–515.
2. Kondo K, Monden Y. A questionnaire about thymic epithelial tumors in Japan. Jpn Assoc Chest Surg 2001;15;633–42.
3. Kanai N, Nagaki S, Tanaka T. Clear cell carcinoma of the pancreas. Acta Pathol Jpn 1987;37;1521–6.
4. Autelinano F, Grillo LR. The clear cell tumor of the thyroid. Recent Progr Med 1981;70;46–69.
5. Hasserjian RP, Klimstra DS, Rosai J. Carcinoma of the thymus with clear-cell features: report of eight cases and review of the literature. Am J Surg Pathol 1995;19;835–41.
6. Hsu CP, Chen CY, Chen CL, Lin CT, Hsu NY, Wang JH, et al. Thymic carcinoma: ten years experience in twenty patients. J Thorac Cardiovasc Surg 1994;197;615–20.
7. Lucchi M, Mussi A, Basolo F, Ambrogi MC, Fontanini G, Angeletti CA. The multimodality treatment of thymic carcinoma. Eur J Cardiothorac Surg 2001;19;566–9.
8. Liu HC, Hsu WH, Chen CL, Chan YJ, Wu YC, Huang BS, et al. Primary thymic carcinoma. Ann Thorac Surg 2002;73; 1076–81.
9. Luciano J. Costa, Harry A. Drabkin. Renal cell carcinoma: new developments in molecular biology and potential for targeted therapies. Oncologist 2007;12;1404–15.

J Anesth (2010) 24:132–133
DOI 10.1007/s00540-009-0844-2

CLINICAL REPORT

Unsuspected tracheal web inhibits endotracheal intubation: report of a case

Shinichi Yamamoto · Kenji Tetsuka · Yukio Sato · Shunsuke Endo

Received: 7 July 2009 / Accepted: 7 September 2009 / Published online: 6 January 2010

Abstract A 66-year-old woman was scheduled for resection of a recurrent brain astrocytoma. During anesthesia induction, endotracheal intubation became impossible. Urgent bronchoscopy under laryngeal mask ventilation visualized a subglottic web 1 cm below the vocal cords. After bronchoscopic ablation with argon plasma coagulation, the airway intubation was successful.

Keywords Tracheal web · Argon plasma coagulation · Laryngeal mask

Introduction

A tracheal web is a rare late complication in endotracheal intubation. Its presence often causes intubation difficulties. We report a case of an asymptomatic subglottic web that blocked endotracheal intubation during general anesthesia for neurosurgery.

Case report

A 66-year-old woman was scheduled for resection of a recurrent brain astrocytoma. The original brain surgery for the astrocytoma had been done under general anesthesia 20 years previously. One year previous to the present operation, the patient had undergone a month of mechanical ventilation as a result of an epileptic attack; endotracheal intubation and tracheostomy were performed at that time. Chest X-ray and respiratory function test before this present surgery showed no abnormal findings. The patient had no respiratory symptoms such as dyspnea or stridor.

On the patient's arrival at the operating room, electrocardiogram, blood pressure, heart rate, and oxygen saturation began to be monitored continuously. After preoxygenation, intravenous induction was accomplished with atropine 0.4 mg, propofol 80 mg, and rocuronium 25 mg. Easy mask ventilation was performed for 2 min. Direct laryngoscopy was accomplished; the laryngoscopic view was grade 1 according to the Cormack and Lehane classification. An initial attempt to pass a 7.0 mm cuffed endotracheal tube beyond the true vocal cords encountered resistance. Similar resistance occurred with endotracheal tube sizes of 6.5 and 6.0 mm. As a tracheal web was confirmed during direct laryngoscopy, two attending anesthesiologists consulted us. Flexible bronchoscopy during laryngeal mask ventilation revealed a tracheal web below the vocal cords (Fig. 1a). It was separated from a tracheostomy scar. Though cancellation of the surgery and tracheostomy was considered, we judged that bronchoscopic ablation was the most appropriate procedure because the area of the tracheal web in the airway was small. After we had obtained informed consent from her family, the web was removed by argon plasma coagulation (APC 300, ERBETOM ICC; Erbe Elektromedizin, Tuebingen, Germany) under flexible bronchoscopy (Fig. 1b). The tracheal web was removed within 10 min without any complications. The patient was subsequently intubated with a 7.0 mm endotracheal tube, and the planned surgery

S. Yamamoto (✉)
Department of General Thoracic Surgery,
Utsunomiya Social Insurance Hospital,
11-17 Minamitakasagotyo, Utsunomiya,
Tochigi 321-0143, Japan
e-mail: tcvyamap@jichi.ac.jp

S. Yamamoto · K. Tetsuka · Y. Sato · S. Endo
Division of General Thoracic Surgery, Department of Surgery,
Jichi Medical University, 3311-1 Yakushiji, Shimotsuke,
Tochigi 329-0498, Japan

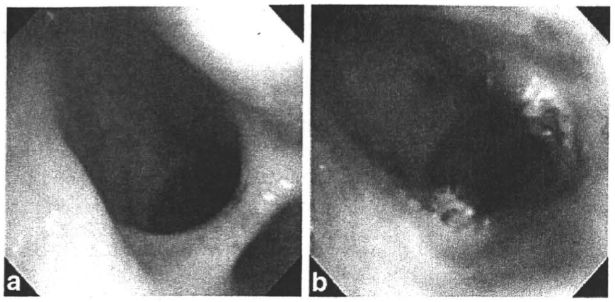

Fig. 1 **a** Bronchoscopic finding: a tracheal web exists below the vocal cords. **b** Bronchoscopic findings after ablation: the tracheal web was removed

proceeded without complications. After the operation, the endotracheal tube was extubated uneventfully. One week later, flexible bronchoscopy confirmed that there was no regrowth of the tracheal web. The patient had no respiratory complications during the rest of her hospital course.

Discussion

In adults, tracheal webs are known as a late complication after endotracheal intubation and after tracheostomy [1, 2], and are characterized as rare [3, 4]. Tracheal webs have been described in children at an incidence of 1 in 10 000 births [3, 4]. The incidence of tracheal webs in adults is unknown. It has been reported that 75% of laryngeal webs occur at the level of the vocal cords, with the remainder being subglottic or supraglottic [3].

The present case was also a complication of endotracheal intubation because the tracheal web was separated from a tracheostomy scar and endotracheal intubation had been possible 1 year previously. Common symptoms of tracheal webs are cough, stridor, and dyspnea on inspiration. Patients are often misdiagnosed as having asthma or chronic obstructive pulmonary disease [5]. However, such symptoms were not seen in this patient and so an evaluation of the airway was not performed before surgery. The area of the tracheal web in the airway was small in this patient, and while it caused no symptoms before surgery, a bridging form of granulation interfered with the endotracheal intubation.

According to the American Society of Anesthesiologists difficult airway algorithm [6], in a patient undergoing general anesthesia who cannot be tracheally intubated, but whose lungs can be ventilated via a mask, the laryngeal mask airway is an alternative to mask ventilation. In the present patient, a laryngeal mask airway was inserted because we needed to remove the tracheal web using a flexible bronchoscope. Bronchoscopic procedures such as ablation and web resection can be performed easily via a laryngeal mask airway [7, 8].

When a tracheal web is small, it can be removed by bronchoscopic ablation. If the area of the tracheal web is large, it may need tracheostomy or even cancellation of the planned surgery. We recommend that otolaryngologists or thoracic surgeons quickly judge whether they can treat the condition immediately if an unexpected tracheal web is found.

References

1. Zias N, Chroneou A, Tabba MK, Gonzalez AV, Gray AW, Lamb CR, et al. Post tracheostomy and post intubation tracheal stenosis: report of 31 cases and review of the literature. BMC Pulm Med. 2008;8:18–26.
2. Brichet A, Verkindre C, Dupont J, Carlier ML, Darras J, Wurtz A, et al. Multidisciplinary approach to management of postintubation tracheal stenoses. Eur Respir J. 1999;13:888–93.
3. Chong ZK, Jawan B, Poon YY, Lee JH. Unsuspected difficult intubation caused by a laryngeal web. Br J Anaesth. 1997;79:396–7.
4. Nguyen NK. Unexpected tracheal web encountered during difficult intubation in the operating room. Proc (Bayl Univ Med Cent). 2006;19:224–5.
5. Legasto AC, Haller JO, Giusti RJ. Tracheal web. Pediatr Radiol. 2004;34:256–8.
6. Benumof JL. Laryngeal mask airway and the ASA difficult airway algorithm. Anesthesiology. 1996;84:686–99.
7. Birmingham B, Mentzer SJ, Body SC. Laryngeal mask airway for therapeutic fiberoptic bronchoscopic procedures. J Cardiothorac Vasc Anesth. 1996;10:519–20.
8. McNamee CJ, Meyns B, Pagliero KM. Flexible bronchoscopy via the laryngeal mask: a new technique. Thorax. 1991;46:141–2.

J. Biochem. 2011;149(1):1–3 doi:10.1093/jb/mvq133

JB THE JOURNAL OF BIOCHEMISTRY

JB Commentary

Arkadia—beyond the TGF-β pathway

Received November 5, 2010; accepted November 16, 2010; published online November 25, 2010

Kohei Miyazono* and Daizo Koinuma

Department of Molecular Pathology, Graduate School of Medicine, University of Tokyo, 7-3-1 Hongo, Bunkyo-ku, Tokyo 113-0033, Japan

*Kohei Miyazono, M.D., Department of Molecular Pathology, Graduate School of Medicine, University of Tokyo, 7-3-1 Hongo, Bunkyo-ku, Tokyo 113-0033, Japan. Tel: +81-3-5841-3345, Fax: +81-3-5841-3354, email: miyazono@m.u-tokyo.ac.jp

Arkadia, also known as ring finger 111 (Rnf111), is an E3 ubiquitin ligase that amplifies transforming growth factor (TGF)-β family signalling through degradation of negative TGF-β signal regulators, i.e. Smad7, c-Ski and SnoN. Arkadia plays critical roles in early embryonic development through modulation of nodal signalling, as well as progression of tissue fibrosis and cancer through regulation of TGF-β signalling. Recent findings suggest that, similar to other ubiquitin ligases, including Smurf1 and 2, Arkadia regulates signalling pathways other than those of the TGF-β family. Arkadia interacts with the clathrin-adaptor 2 (AP2) complex and regulates endocytosis of certain cell surface receptors, leading to modulation of epidermal growth factor (EGF) and possibly other signalling pathways.

Keywords: TGF-β/EGF/ubiquitin ligase/AP2 complex/endocytosis.

Abbreviations: AP2, clathrin-adaptor 2; EGF, epidermal growth factor; EMT, epithelial-mesenchymal transition; R-Smads, receptor-regulated Smads; TGF-β, transforming growth factor-β.

Arkadia is an E3 ubiquitin ligase, and was originally identified as a molecule that amplifies nodal signalling. Nodal is a member of the transforming growth factor-β (TGF-β) family, which is structurally similar to activin. Formation of the node, the equivalent of *Xenopus* Spemann's organizer in mammalian embryos, plays an essential role in specification of the axis during early embryonic development. Using gene-trap mutageneis, Episkopou and colleagues (*1*, *2*) discovered Arkadia as a molecule responsible for induction of the node through enhancement of nodal signalling.

TGF-β family signalling is transduced through Smad and non-Smad pathways (*3*, *4*). Arkadia is an intracellular protein containing a RING finger domain, and has been shown to enhance TGF-β family signalling through ubiquitin-dependent degradation of some intracellular proteins. Smad7, an inhibitory Smad, suppresses TGF-β family signalling through multiple mechanisms, including physical interaction with type I receptors for TGF-β family proteins, resulting in blockade of activation of receptor-regulated Smads (R-Smads; Smad2 and Smad3 for TGF-β, activin and nodal signalling) (*4*). Arkadia physically interacts with Smad7, induces ubiquitin-dependent degradation of it, and thereby enhances TGF-β family signalling (*5*). In addition to Smad7, Arkadia has been reported to induce degradation of phospho-Smad2/3, which may lead to efficient and maximal nodal signalling for rapid resetting of target gene promoters (*6*).

In addition, TGF-β family signalling is suppressed by the transcriptional co-repressor c-Ski and its related protein SnoN in the nucleus (*4*). c-Ski and SnoN have been reported to interfere with the interaction of R-Smads with transcriptional co-activators p300 and CBP, recruit histone deacetylases to Smad complexes, and disrupt the formation of Smad complexes, leading to attenuation of TGF-β family signalling. Arkadia binds to c-Ski and SnoN, and down-regulates the levels of their expression through ubiquitin-dependent degradation (*7*–*9*).

Since Arkadia enhances TGF-β family signalling, it plays pivotal roles in progression of various diseases in which TGF-β family signalling is involved. TGF-β induces tissue fibrosis, suggesting that Arkadia may be involved in the pathogenesis of some fibrotic disorders. Liu *et al.* reported that levels of expression of mRNAs for type 1 collagen, TGF-β1, TGF-β type I receptor, Smad7 and Arkadia were increased in a rat model of tubulointerstitial fibrosis, while that of Smad7 protein was decreased in the kidney. They suggested that Arkadia may play a major role in degradation of Smad7, induction of epithelial-mesenchymal transition (EMT) of tubular epithelial cells, and progression of tubulointerstitial fibrosis (*10*, *11*). In support of these findings, Gai *et al.* (*12*) reported that in *Trps1* haploinsufficiency mice (TRPS1 encodes a transcription factor and is responsible for tricho-rhino-pharyngeal syndrome), tubulointerstitial fibrosis was induced by increased phosphorylation of Smad3 and decreased expression of Smad7 protein. They also found that the level of expression of Arkadia was increased in the proximal tubule cells of $Trps1^{+/-}$ mice, and suggested that Arkadia played an essential role in the induction of EMT in these cells.

The function of Arkadia may also be linked to progression of cancer. Through induction of the degradation of c-Ski, Arkadia accelerates tumor metastasis of breast and lung cancer cells in mice, possibly by induction of EMT (*9*). A study using 20 human cancer cell lines revealed ubiquitous expression of Arkadia (*13*).

Levels of expression of c-Ski and SnoN proteins varied markedly and did not correlate with those of Arkadia protein in these cells. In some cancer cell lines, including diffuse-type gastric cancer OCUM-2MLN, Arkadia failed to degrade c-Ski protein, suggesting dysfunction of it in certain cancer cells. Since TGF-β signalling interferes with the progression of diffuse-type gastric cancer OCUM-2MLN *in vivo* (*14*), perturbations of the function of Arkadia may accelerate the progression of this type of cancer.

Smurf1 and 2 were originally identified as HECT type E3 ubiquitin ligases able to induce degradation of R-Smads and suppress TGF-β family signalling. Smurf1/2 also interact with inhibitory Smads (Smad6 and 7) and degrade type I receptors for the TGF-β family proteins. Smurfs thus exhibit biological activities opposite to those of Arkadia. However, it has been found that the targets of Smurfs are not restricted to the TGF-β family signalling proteins, and that they induce degradation of many other proteins, *e.g.* Runx2, RhoA, MEKK2, Axin and p53 (*15*, *16*).

Similar to Smurf proteins, Mizutani *et al.* (*17*) found that the function of Arkadia is not limited to regulation of TGF-β family signalling. Through yeast-two-hybrid screening, the μ2 subunit of clathrin-adaptor 2 (AP2) complex was identified as an Arkadia-interacting protein. The AP2 complex plays an essential role in the endocytotic machinery that links cargo membrane proteins to the clathrin lattice (*18*). The AP2 complex is composed of four subunits, *i.e.* α, β2, μ2 and σ2. The N-terminal portion of the μ2 subunit is known to be located at the centre of the AP2 complex, while the C-terminal domain of μ2 has been shown to physically interact with Arkadia (*17*). Arkadia induced ubiquitination of the μ2 subunit, and regulated endocytosis of epidermal growth factor (EGF) receptor induced by EGF (Fig. 1). Arkadia may thus regulate a wide variety of signalling processes, in which endocytosis of the cell surface receptors is regulated by the AP2 complex. Since Arkadia-null mice are embryonic lethal, analyses of conditional knockout mice lacking expression of Arkadia in certain tissues may disclose novel *in vivo* functions of Arkadia.

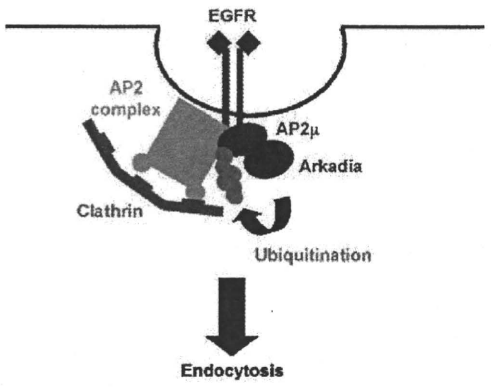

Fig. 1 Regulation of endocytosis of EGF receptor (EGFR) by Arkadia-AP2 complex. Currently, it is unknown whether AP2μ interacts with EGFR and Arkadia at the same time.

References

1. Episkopou, V., Arkell, R., Timmons, P.M., Walsh, J.J., Andrew, R.L., and Swan, D. (2001) Induction of the mammalian node requires Arkadia function in the extra-embryonic lineages. *Nature* **410**, 825–830
2. Niederländer, C., Walsh, J.J., Episkopou, V., and Jones, C.M. (2001) Arkadia enhances nodal-related signalling to induce mesendoderm. *Nature* **410**, 830–834
3. Feng, X.H. and Derynck, R. (2005) Specificity and versatility in TGF-β signaling through Smads. *Annu. Rev. Cell Dev. Biol.* **21**, 659–693
4. Miyazono, K., Kamiya, Y., and Morikawa, M. (2010) Bone morphogenetic protein receptors and signal transduction. *J. Biochem.* **147**, 35–51
5. Koinuma, D., Shinozaki, M., Komuro, A., Goto, K., Saitoh, M., Hanyu, A., Ebina, M., Nukiwa, T., Miyazawa, K., Imamura, T., and Miyazono, K. (2003) Arkadia amplifies TGF-β superfamily signalling through degradation of Smad7. *EMBO J.* **22**, 6458–6470
6. Mavrakis, K.J., Andrew, R.L., Lee, K.L., Petropoulou, C., Dixon, J.E., Navaratnam, N., Norris, D.P., and Episkopou, V. (2007) Arkadia enhances Nodal/TGF-β signaling by coupling phospho-Smad2/3 activity and turnover. *PLoS Biol.* **5**, e67
7. Nagano, Y., Mavrakis, K.J., Lee, K.L., Fujii, T., Koinuma, D., Sase, H., Yuki, K., Isogaya, K., Saitoh, M., Imamura, T., Episkopou, V., Miyazono, K., and Miyazawa, K. (2007) Arkadia induces degradation of SnoN and c-Ski to enhance transforming growth factor-β signaling. *J. Biol. Chem.* **282**, 20492–20501
8. Levy, L., Howell, M., Das, D., Harkin, S., Episkopou, V., and Hill, C.S. (2007) Arkadia activates Smad3/Smad4-dependent transcription by triggering signal-induced SnoN degradation. *Mol. Cell. Biol.* **27**, 6068–6083
9. Le Scolan, E., Zhu, Q., Wang, L., Bandyopadhyay, A., Javelaud, D., Mauviel, A., Sun, L., and Luo, K. (2008) Transforming growth factor-β suppresses the ability of Ski to inhibit tumor metastasis by inducing its degradation. *Cancer Res.* **68**, 3277–3285
10. Liu, F.Y., Li, X.Z., Peng, Y.M., Liu, H, and Liu, Y.H. (2007) Arkadia-Smad7-mediated positive regulation of TGF-β signaling in a rat model of tubulointerstitial fibrosis. *Am. J. Nephrol.* **27**, 176–183
11. Liu, F.Y., Li, X.Z., Peng, Y.M., Liu, H., and Liu, Y.H. (2008) Arkadia regulates TGF-β signaling during renal tubular epithelial to mesenchymal cell transition. *Kidney Int.* **73**, 588–594
12. Gai, Z., Zhou, G., Gui, T., Itoh, S., Oikawa, K., Uetani, K., and Muragaki, Y. (2010) Trps1 haploinsufficiency promotes renal fibrosis by increasing Arkadia expression. *J. Am. Soc. Nephrol.* **21**, 1468–1476
13. Nagano, Y., Koinuma, D., Miyazawa, K., and Miyazono, K. (2010) Context-dependent regulation of the expression of c-Ski protein by Arkadia in human cancer cells. *J. Biochem.* **147**, 545–554
14. Komuro, A., Yashiro, M., Iwata, C., Morishita, Y., Johansson, E., Matsumoto, Y., Watanabe, A., Aburatani, H., Miyoshi, H., Kiyono, K., Shirai, Y., Suzuki, H.I., Hirakawa, K., Kano, M.R., and Miyazono, K. (2009) Diffuse-type gastric carcinoma: Progression, angiogenesis, and transforming growth factor-β signaling. *J. Natl. Cancer Inst.* **101**, 592–604

15. Miyazono, K. (2008) Regulation of TGF-β family signaling by I-Smads in *The TGF-β Family* (Derynck, R. and Miyazono, K., eds.), pp. 363–387, Cold Spring Harbor Laboratory Press, New York
16. Andrews, P.S., Schneider, S., Yang, E., Michaels, M., Chen, H., Tang, J., and Emkey, R. (2010) Identification of substrates of SMURF1 ubiquitin ligase activity utilizing protein microarrays. *Assay Drug Dev. Technol.* **8**, 471–487
17. Mizutani, A., Saitoh, M., Imamura, T., Miyazawa, K., and Miyazono, K. (2010) Arkadia complexes with clathrin adaptor AP2 and regulates EGF signaling. *J. Biochem* **148**, 733–741
18. Ohno, H. (2006) Clathrin-associated adaptor protein complexes. *J. Cell. Sci.* **119**, 3719–3721

Oncogene (2010), 1–13

www.nature.com/onc

ORIGINAL ARTICLE

Transforming growth factor-β decreases the cancer-initiating cell population within diffuse-type gastric carcinoma cells

S Ehata[1,2], E Johansson[1], R Katayama[2], S Koike[2], A Watanabe[3], Y Hoshino[1], Y Katsuno[1], A Komuro[1], D Koinuma[1], MR Kano[1], M Yashiro[4], K Hirakawa[4], H Aburatani[3], N Fujita[2] and K Miyazono[1]

[1]Department of Molecular Pathology, Graduate School of Medicine, University of Tokyo, 7-3-1 Hongo, Bunkyo-ku, Tokyo, Japan; [2]Cancer Chemotherapy Center, Japanese Foundation for Cancer Research (JFCR), 3-10-6 Ariake, Koto-ku, Tokyo, Japan; [3]Genome Science Division, Research Center for Advanced Science and Technology, University of Tokyo, 4-6-1 Komaba, Meguro-ku, Tokyo, Japan and [4]Department of Surgical Oncology, Graduate School of Medicine, Osaka City University, 1-4-3 Asahi-machi, Abeno-ku, Osaka, Japan

Stem cells in normal tissues and cancer-initiating cells (CICs) are known to be enriched in side population (SP) cells. However, the factors responsible for the regulation of expression of ABCG2, involved in efflux of dyes, in SP cells have not been fully investigated. Here, we characterized the SP cells within diffuse-type gastric carcinoma, and examined the effects of transforming growth factor-β (TGF-β) on SP cells. Diffuse-type gastric carcinoma cells established from four independent patients universally contained SP cells between 1 and 4% of total cells, which displayed greater tumorigenicity than non-SP cells did. TGF-β repressed the transcription of ABCG2 through direct binding of Smad2/3 to its promoter/enhancer, and the number of SP cells and the tumor-forming ability of cancer cells were decreased by TGF-β, although ABCG2 is not directly involved in the tumor-forming ability of SP cells. Cancer cells from metastatic site expressed much higher levels of ABCG2 and included a greater percentage of SP cells than parental cancer cells did. SP cells are thus responsible for the progression of diffuse-type gastric carcinoma, and TGF-β negatively contributes to maintain the CICs within the cancer.
Oncogene advance online publication, 6 December 2010; doi:10.1038/onc.2010.546

Keywords: ABCG2; cancer-initiating cell; diffuse type gastric carcinoma; SP cell; TGF-β

Introduction

Gastric cancer remains a major public health issue as the fourth most common cancer and the second leading cause of cancer death worldwide (Hohenberger and Gretschel, 2003; Crew and Neugut, 2006). Of the two histological subtypes of gastric cancers, the incidence of proximal, diffuse-type gastric adenocarcinoma has been increasing, particularly in Western countries. Diffuse-type gastric carcinoma is an aggressive type of gastric cancer with poor prognosis, affecting relatively young individuals. The majority of diffuse-type gastric carcinomas are in advanced stages, for which gastrectomy and chemotherapy are of limited efficacy. Thus, understanding of the mechanism underlying progression of diffuse-type gastric carcinoma is essential for management of this tumor.

The concept of 'cancer stem cells' or 'cancer-initiating cells (CICs)' is an attractive explanation for the functional heterogeneity that is commonly observed in many types of tumors. Tumors possess a hierarchical organization of cells, among which a subpopulation of stem-like cells is responsible for sustaining tumor growth (Stingl and Caldas, 2007; Visvader and Lindeman, 2008). As these cells are likely to share many of the properties of normal stem cells, which have a long lifespan, self-renewal ability, resistance to drugs, active DNA-repair activity and resistance to apoptosis, the presence of CICs is thought to be important for progression of tumors and resistance to conventional therapies (Dean *et al.*, 2005). Recently, CICs have been identified in a range of hematopoietic malignancies and solid tumors (Bonnet and Dick, 1997; Lobo *et al.*, 2007). In the maintenance of CICs, the interaction of CICs and 'niche' has critical roles, and factors secreted from the tumor microenvironment appear to regulate the maintenance of CICs in certain niches (Iwasaki and Suda, 2009). However, the factors responsible for regulation of the CIC pool have not been fully investigated.

Transforming growth factor-β (TGF-β) is the prototypic member of a family of secreted proteins that includes three isoforms of TGF-β (TGF-β1, TGF-β2 and TGF-β3), activins and bone morphogenetic proteins (BMPs). TGF-β mediates biological activities in cells through binding to heteromeric complexes of receptors on the cell surface that are composed of TGF-β type I and type II (TβRII) receptors. TGF-β type I receptor activated by TβRII phosphorylates Smad2 and Smad3, which interact with Smad4 and translocate to the

Correspondence: Professor K Miyazono, Department of Molecular Pathology, Graduate School of Medicine, University of Tokyo, 7-3-1 Hongo, Bunkyo-ku, Tokyo 113-0033, Japan.
E-mail: miyazono@m.u-tokyo.ac.jp
Received 10 August 2010; revised 15 October 2010; accepted 20 October 2010

nucleus. Nuclear Smad2/3–Smad4 complexes bind to transcription factors and transcriptional co-activators/repressors, and regulate transcription of target genes (Miyazawa *et al.*, 2002; Derynck and Zhang, 2003; Massagué, 2008). In epithelial cells, TGF-β inhibits cell proliferation, induces apoptosis and mediates differentiation, suggesting that components of the TGF-β signaling pathways have tumor-suppressive activity in epithelial tumors (Wakefield and Roberts, 2002; Bierie and Moses, 2006). Accordingly, mutations of TβRII, TGF-β type I receptor, Smad4 and Smad2, have been reported to be responsible for progression of cancers, particularly gastrointestinal tumors (Bierie and Moses, 2006).

We previously reported that deregulation of the TGF-β signaling pathway in the diffuse-type gastric carcinoma OCUM-2MLN cells, which were derived from lymph node metastasis of orthotopically implanted primary carcinoma cells, promotes the growth of primary tumors in mouse xenograft models through acceleration of angiogenesis (Kiyono *et al.*, 2009; Komuro *et al.*, 2009). In addition to this mechanism, we here present evidence that TGF-β has a novel role in regulation of the maintenance of CICs in diffuse-type gastric carcinoma cells. Our observations provide new insights into the molecular mechanisms governing TGF-β-mediated regulation of gastric carcinogenesis and may support the development of new strategies for the treatment of diffuse-type gastric carcinoma.

Results

CICs are enriched in 2MLN-dnTβRII cells

Tumor growth of diffuse-type gastric carcinoma OCUM-2MLN cells is reported to be enhanced by inhibition of the TGF-β signaling pathway in cancer cells (Kiyono *et al.*, 2009; Komuro *et al.*, 2009). In accordance with these reports, TGF-β-induced phosphorylation of Smad2 was completely inhibited in OCUM-2MLN cells, which stably expressed dominant negative form of TβRII (2MLN-dnTβRII), but not in control cells, which expressed green fluorescent protein (2MLN-GFP) (Figure 1a). TGF-β inhibited the proliferation of keratinocyte HaCaT cells *in vitro*, whereas TGF-β did not affect the rate of growth of the OCUM-2MLN cells (Figure 1b). Cells enter the S phase and proliferate when the phosphorylated retinoblastoma protein (RB) is hyperphosphorylated, whereas cells are arrested in G1 when phosphorylated RB is hypophosphorylated (Weinberg, 1995). Treatment of HaCaT cells with TGF-β decreased hyperphosphorylated RB expression, whereas hyperphosphorylated RB expression in OCUM-2MLN cells was not altered by TGF-β (Figure 1c). In contrast to *in vitro* cell proliferation, *in vivo* tumor growth of 2MLN-dnTβRII cells was accelerated in the subcutaneous mouse tumor model compared with that of 2MLN-GFP cells (Figure 1d). In the previous study, we showed that angiogenesis was accelerated in 2MLN-dnTβRII tumors through repression of the expression of the anti-angiogenic factor thrombospondin-1 (Komuro *et al.*, 2009). However, thrombospondin-1 expression is not sufficient to account for all the histological change in tumor obtained by the overexpression of dnTβRII, such as the accumulation of fibrotic tissues. Thus, we attempted here to uncover additional underlying mechanisms by which the deregulation of TGF-β signaling in OCUM-2MLN cells promotes *in vivo* tumor growth, and especially focused on the heterogeneity of cancer cells.

We examined whether 2MLN-dnTβRII cells include a higher proportion of CICs than 2MLN-GFP cells do. Various amounts of 2MLN-GFP and 2MLN-dnTβRII cells were injected into nude mice and compared for tumor-forming ability (Figure 1e). In 2MLN-dnTβRII cells, subcutaneous tumor formation required injection of 1×10^3 cells, whereas injection of 3×10^3 2MLN-GFP cells constantly failed to induce tumor formation in all mice examined ($n = 4$). These findings suggested that 2MLN-dnTβRII cells promote tumor formation through enrichment of CICs in cancer cells.

ABCG2 is highly expressed in 2MLN-dnTβRII tumors

We hypothesized that TGF-β from the tumor microenvironment decreases the tumor-forming ability of OCUM-2MLN cells *in vivo*. To examine the alterations caused by disruption of the TGF-β signaling pathway in diffuse-type gastric carcinoma cells *in vivo*, we made use of comprehensive gene expression data sets for these tumors previously obtained using oligonucleotide microarray analysis (Komuro *et al.*, 2009). In our previous study, DAVID functional annotation clustering revealed that the expression of thrombospondin-1 in tumor tissues was increased by TGF-β, and thrombospondin-1 was reported as one of the 'TGF-β-positively regulated genes' in OCUM-2MLN cells (Dennis *et al.*, 2003). However, novel candidate gene(s) related to the 'tumor-forming ability' or 'stemness' of 2MLN-dnTβRII cells was not picked up among these 'TGF-β-positively regulated genes'. Thus, genes that were strongly expressed in 2MLN-dnTβRII tumors, namely 'TGF-β-negatively regulated genes', were focused, and identified as shown in Figure 2a.

Among the 30 genes upregulated in 2MLN-dnTβRII tumors, ATP-binding cassette G2 (ABCG2) was included (Figure 2a). ABCG2 contributes to efflux of many types of dyes, including Hoechst 33342. Although uptake of Hoechst 33342 occurs universally in all cells, efflux of it is less common. Cells with efflux capacity conferred by ABCG2 expression are negatively stained on flow cytometric analysis, and referred to as side population (SP) cells on dot plots. As ABCG2 expression and SP cells are thought to be of importance in the isolation of CICs (Wu and Alman, 2008), we focused on the function of ABCG2.

TGF-β regulates the transcription of ABCG2 through the Smad pathway

First, we examined whether ABCG2 is one of the downstream targets of TGF-β in OCUM-2MLN cells by quantitative real-time reverse transcription–PCR

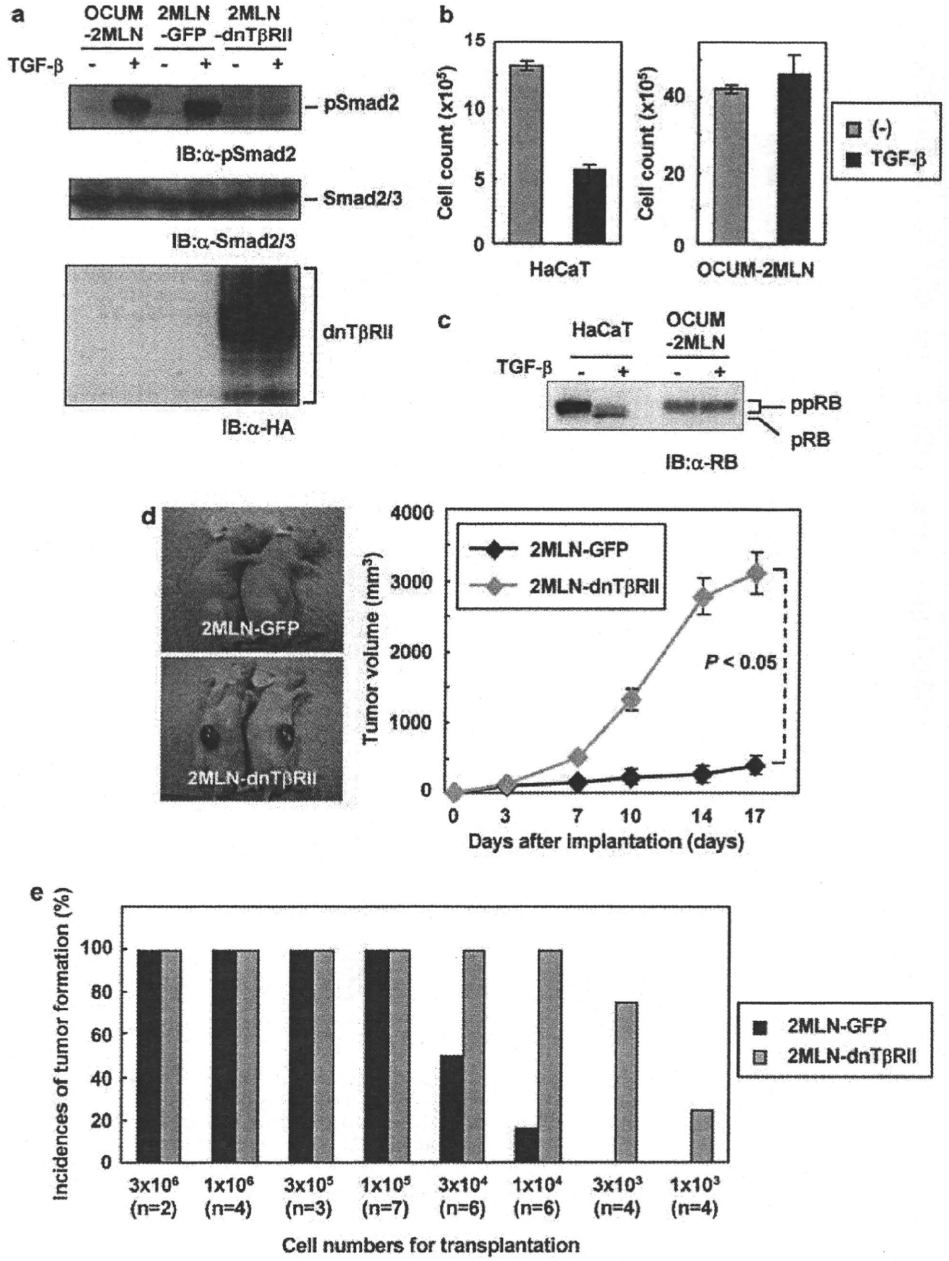

Figure 1 CICs are enriched in 2MLN-dnTβRII cells. (**a**) OCUM-2MLN cells were infected with lentiviruses carrying GFP cDNA (2MLN-GFP) and dnTβRII cDNA (2MLN-dnTβRII), and treated with TGF-β (1 ng/ml) for 1 h. Cell lysates were subjected to immunoblotting with indicated antibodies. (**b**) HaCaT and OCUM-2MLN cells were treated with TGF-β (1 ng/ml) for 4 days, and counted. *Columns*, mean of duplicate determinations; *bars*, s.d. (**c**) Hyperphosphorylation of pRB in the cells in (**b**) was determined with anti-phospho-pRB antibody. RB proteins migrate as multiple bands because of varying degrees of phosphorylation. (**d**) A total of 3×10^6 OCUM-2MLN or 2MLN-dnTβRII cells were xenografted. Representative photographs (*left panels*) and tumor volumes (*right panel*) were indicated. *Points*, mean; *bars*, s.d. (**e**) The indicated numbers of 2MLN-GFP or 2MLN-dnTβRII cells were injected into BALB/c *nu/nu* mice. Incidences of tumor formation 4 weeks after injection are shown.

(RT–PCR) (Figure 2b). Expression of ABCG2 was downregulated in response to exogenous TGF-β in parental OCUM-2MLN and 2MLN-GFP cells, whereas similar repression was not apparent in 2MLN-dnTβRII cells. We also demonstrated that treatment with TGF-β, but not with BMP-4, downregulated the *ABCG2* messenger RNA (Figure 3a) and ABCG2 protein (Figure 3b) in OCUM-2MLN cells.

In order to confirm the involvement of the Smad-dependent signal transduction by TGF-β, we knocked

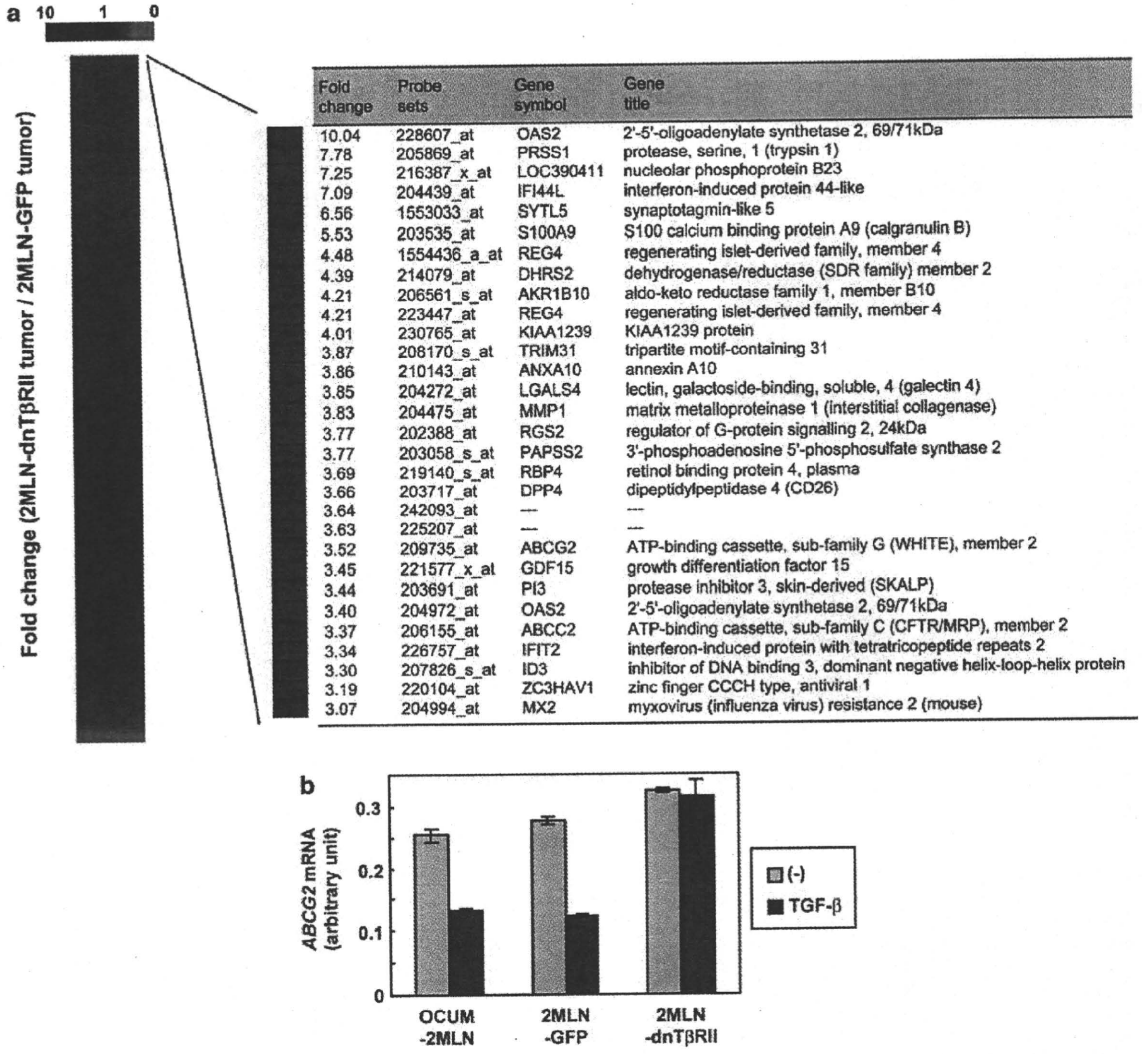

Fold change	Probe sets	Gene symbol	Gene title
10.04	228607_at	OAS2	2'-5'-oligoadenylate synthetase 2, 69/71kDa
7.78	205869_at	PRSS1	protease, serine, 1 (trypsin 1)
7.25	216387_x_at	LOC390411	nucleolar phosphoprotein B23
7.09	204439_at	IFI44L	interferon-induced protein 44-like
6.56	1553033_at	SYTL5	synaptotagmin-like 5
5.53	203535_at	S100A9	S100 calcium binding protein A9 (calgranulin B)
4.48	1554436_a_at	REG4	regenerating islet-derived family, member 4
4.39	214079_at	DHRS2	dehydrogenase/reductase (SDR family) member 2
4.21	206561_s_at	AKR1B10	aldo-keto reductase family 1, member B10
4.21	223447_at	REG4	regenerating islet-derived family, member 4
4.01	230765_at	KIAA1239	KIAA1239 protein
3.87	208170_s_at	TRIM31	tripartite motif-containing 31
3.86	210143_at	ANXA10	annexin A10
3.85	204272_at	LGALS4	lectin, galactoside-binding, soluble, 4 (galectin 4)
3.83	204475_at	MMP1	matrix metalloproteinase 1 (interstitial collagenase)
3.77	202388_at	RGS2	regulator of G-protein signalling 2, 24kDa
3.77	203058_s_at	PAPSS2	3'-phosphoadenosine 5'-phosphosulfate synthase 2
3.69	219140_s_at	RBP4	retinol binding protein 4, plasma
3.66	203717_at	DPP4	dipeptidylpeptidase 4 (CD26)
3.64	242093_at	---	---
3.63	225207_at	---	---
3.52	209735_at	ABCG2	ATP-binding cassette, sub-family G (WHITE), member 2
3.45	221577_x_at	GDF15	growth differentiation factor 15
3.44	203691_at	PI3	protease inhibitor 3, skin-derived (SKALP)
3.40	204972_at	OAS2	2'-5'-oligoadenylate synthetase 2, 69/71kDa
3.37	206155_at	ABCC2	ATP-binding cassette, sub-family C (CFTR/MRP), member 2
3.34	226757_at	IFIT2	interferon-induced protein with tetratricopeptide repeats 2
3.30	207826_s_at	ID3	inhibitor of DNA binding 3, dominant negative helix-loop-helix protein
3.19	220104_at	ZC3HAV1	zinc finger CCCH type, antiviral 1
3.07	204994_at	MX2	myxovirus (influenza virus) resistance 2 (mouse)

Figure 2 *ABCG2* is highly expressed in 2MLN-dnTβRII tumors. (**a**) Gene expression in 2MLN-GFP and 2MLN-dnTβRII tumors was analyzed on the GeneChip Human Genome U133 Plus 2.0 Array. Genes strongly expressed in 2MLN-dnTβRII tumors were purified as follows: (1) Signal intensities in 2MLN-dnTβRII were >100, and given 'PRESENT' calls: 13208 probe sets met this restriction. (2) Signals intensities in 2MLN-dnTβRII were increased more than threefold, compared with signal intensities in 2MLN-GFP: 30 of the 13208 probe sets met this restriction, all of which are listed. (**b**) OCUM-2MLN, 2MLN-GFP and 2MLN-dnTβRII cells were treated with TGF-β (1 ng/ml) for 24 h, and expression of *ABCG2* mRNA was examined by quantitative real-time RT–PCR. *Columns*, mean; *bars*, s.d.

down the endogenous expression of Smad4. Smad4 expression in OCUM-2MLN cells was successfully silenced by small interfering RNA (siRNA) targeting Smad4 (Figure 3c), and TGF-β-induced ABCG2 reduction was abolished by Smad4 knockdown, indicating that TGF-β regulates the expression of ABCG2 through the Smad-dependent pathway. Though downregulation of *ABCG2* messenger RNA by TGF-β in OCUM-2MLN cells was augmented at 8 h treatment with TGF-β, slight decrease in the expression of *ABCG2* messenger RNA was already observed only after the first 1 h (Figure 3a). Furthermore, the decrease in expression of ABCG2 by TGF-β was not abolished by suppression of *de novo* protein synthesis by treatment of OCUM-2MLN cells with cycloheximide (Figure 3d). To determine whether ABCG2 is a direct target of TGF-β in OCUM-2MLN cells, we performed chromatin immunoprecipitation using antibody against Smad2/3, DNA-binding mediators of Smad-dependent signal transduction. We have demonstrated that activated Smad2/3 directly bound to the promoter elements located in 200 bp upstream of the start point of transcription of *ABCG2* and also bound to the enhancer element located in the first intron of *ABCG2* in response

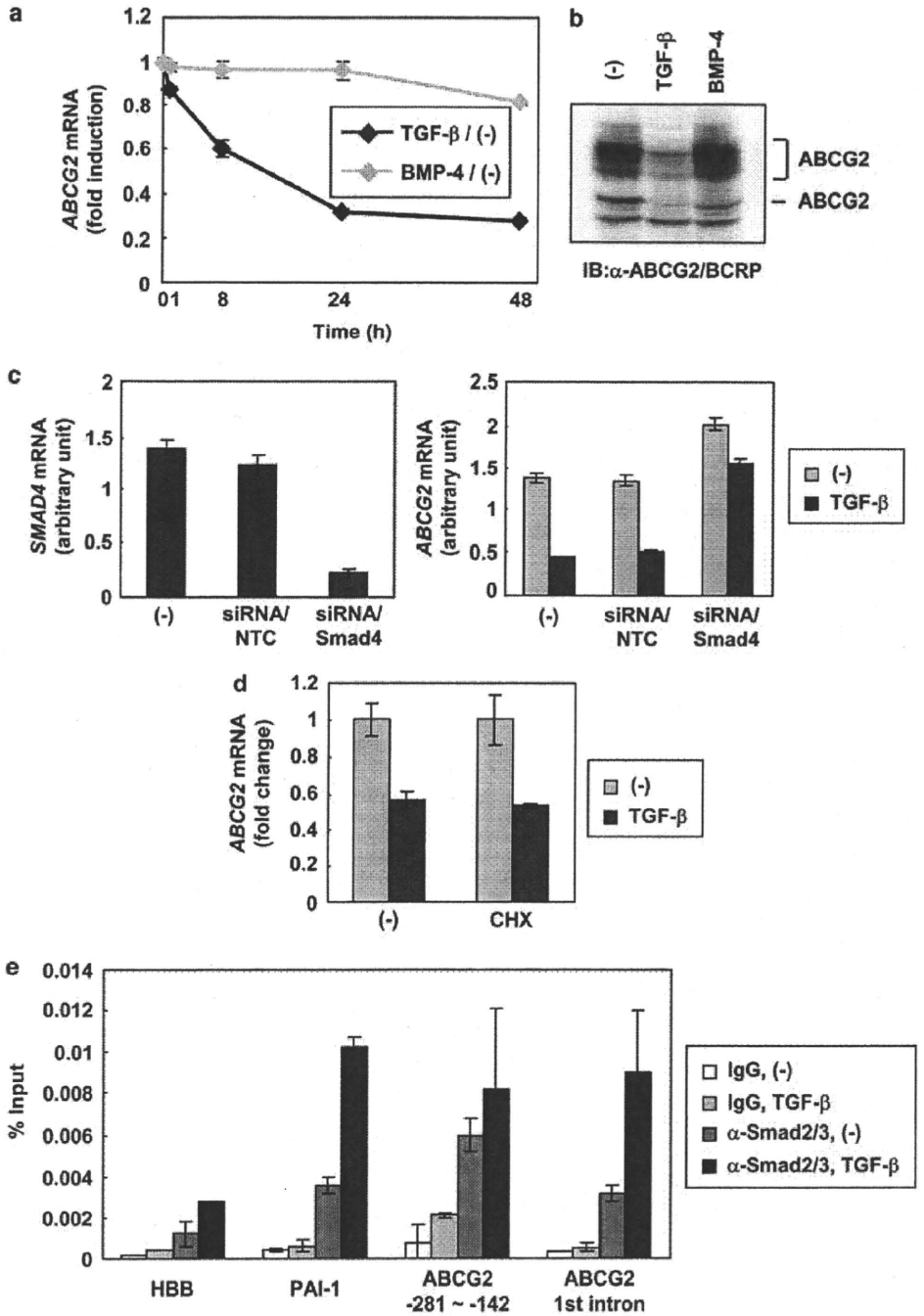

Figure 3 ABCG2 is a direct target of TGF-β. (**a**) OCUM-2MLN cells were treated with TGF-β (1 ng/ml) or BMP-4 (30 ng/ml). Expression of *ABCG2* mRNA at the indicated time points was examined by quantitative real-time RT–PCR. Fold-induction by TGF-β or BMP-4 stimulation is indicated. *Points*, mean. (**b**) OCUM-2MLN cells were stimulated with TGF-β (1 ng/ml) or BMP-4 (30 ng/ml) for 72 h, and expression of ABCG2 protein was examined by immunoblotting using anti-ABCG2/BCRB antibody. (**c**) OCUM-2MLN cells were transfected in the presence of either siRNA/Smad4 or control siRNA/NTC. At 9 h after transfection, cells were treated with TGF-β (1 ng/ml) for further 40 h. Levels of expression of *SMAD4* mRNA and *ABCG2* mRNA were determined by quantitative real-time RT–PCR. *Columns*, mean; *bars*, s.d. (**d**) OCUM-2MLN cells were treated with TGF-β (1 ng/ml) in the absence or presence of cycloheximide (CHX) (1 μg/ml). Total RNA was extracted 24 h after stimulation, and expression of *ABCG2* mRNA were examined by quantitative real-time RT–PCR. Fold-induction by TGF-β stimulation is indicated. *Columns*, mean; *bars*, s.d. (**e**) Association of the Smad complex with the ABCG2 promoter/enhancer elements. OCUM-2MLN cells were treated with TGF-β (1 ng/ml). Chromatin immunoprecipitation using anti-Smad2/3 antibody was preformed. Smad2/3-bound DNAs at 1.5 h after TGF-β treatment were examined by quantitative real-time RT–PCR using indicated primers. *Columns*, mean; *bars*, s.d.

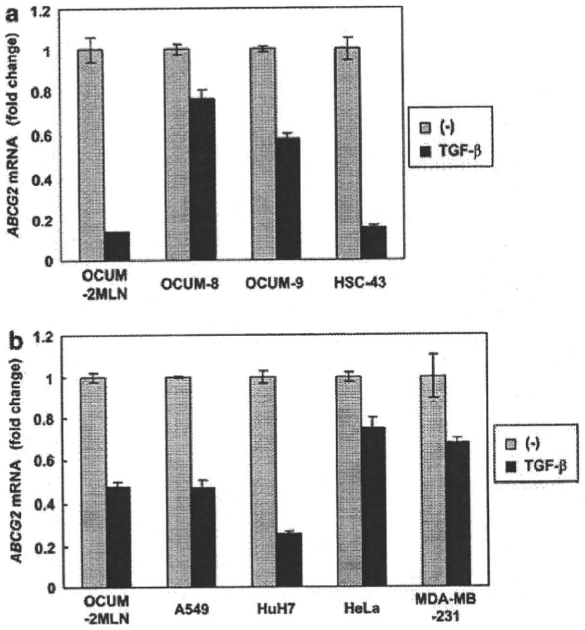

Figure 4 TGF-β regulates the transcription of ABCG2 in various cancers. **(a)** Diffuse-type gastric carcinoma cells were treated with TGF-β (1 ng/ml) for 72 h. Expression of *ABCG2* mRNA was examined by quantitative real-time RT–PCR. Fold-induction by TGF-β stimulation is indicated. *Columns*, mean; *bars*, s.d. **(b)** The indicated cancer cells were treated with TGF-β (1 ng/ml) for 72 h. Expression of *ABCG2* mRNA was examined by quantitative real-time RT–PCR. Fold-induction by TGF-β stimulation is indicated. *Columns*, mean; *bars*, s.d.

to TGF-β (Figure 3e). Taken together, these findings indicate that ABCG2 is a direct target gene of TGF-β signaling.

Transcriptional regulation of ABCG2 by TGF-β was also examined using other diffuse-type gastric carcinoma cells established form other patients, including OCUM-8, OCUM-9 and HSC-43 cells (Figure 4a). Quantitative real-time RT–PCR revealed decrease in ABCG2 expression by TGF-β in these cells, although degrees of the decrease in ABCG2 expression were variable. Moreover, similar to OCUM-2MLN cells, downregulation of ABCG2 by exogenous TGF-β was commonly observed in neoplasm arising in other organs, including lung, liver, uterus and mammary glands (Figure 4b).

SP cells display tumorigenic property

To confirm whether ABCG2 transporter was functional in OCUM-2MLN cells, we tested for the presence of SP cells in OCUM-2MLN cells by staining with Hoechst 33342. OCUM-2MLN cells included a distinct fraction of SP cells, comprising 1.42% of the total cell population, which was decreased by pretreatment with transporter inhibitors, verapamil, reserpine or fumitremorgin C (Figure 5a). Among many types of ABC transporters, ABCG2 activity is known to be completely inhibited by fumitremorgin C (Rabindran *et al.*, 2000), indicating that ABCG2 expressed in SP cells is critical for the efflux of Hoechst 33342. In agreement with this finding, knockdown of ABCG2 expression in OCUM-2MLN cells resulted in the decrease in the number of SP cells (data not shown).

Next, to examine the characteristics of SP cells, we sorted the SP cells (Figure 5b) and cultured *in vitro* for 7 days. Then, cells were re-stained with Hoechst 33342 and subjected to flow cytometric analysis. SP cells reproduced both SP cells and non-SP cells, indicating that the SP cells within OCUM-2MLN cells had repopulating capacity.

To directly determine whether CICs are enriched in SP cells *in vivo*, equal numbers of SP cells or non-SP cells were transplanted into nude mice. Tumor volume of SP cell-xenografted mice was statistically significantly larger than that of non-SP cell-xenografted mice (Figure 5c). These findings suggested that the OCUM-2MLN cells consist of heterogeneous cell populations, and that SP cells have a more important role than non-SP cells in the tumor formation by OCUM-2MLN cells as 'CICs' within cancer tissues.

TGF-β diminishes the SP fraction of OCUM-2MLN cells

As SP cells appear to be of crucial importance for tumor formation *in vivo*, we hypothesized that TGF-β diminishes the SP fraction of OCUM-2MLN cells through repression of ABCG2 transcription. To test this hypothesis, we prepared OCUM-2MLN cells pretreated with TGF-β or BMP-4 and characterized them. As expected, flow cytometric analysis demonstrated that TGF-β, but not BMP-4, diminished the SP fraction of OCUM-2MLN cells (Figure 6a). TGF-β-mediated regulation of SP cells was also observed in other diffuse-type gastric carcinoma cells (Figure 6b). These results were correlated to the expression of ABCG2 (Figures 3a and 4a).

Next, we examined whether TGF-β decreases the tumor-forming potential of OCUM-2MLN cells *in vitro* and *in vivo*. Colony formation of OCUM-2MLN cells was inhibited by treatment with TGF-β (Figure 6c). In a mouse xenograft experiment, subcutaneous tumor was formed by the injection of 1×10^5 control cells, while TGF-β-treated cells exhibited limited tumorigenesity even if the same amounts of control cells were injected (Figure 6d). These findings suggested that TGF-β decreased the SP fraction of OCUM-2MLN cells, and thereby attenuated the tumor-forming ability of OCUM-2MLN cells.

Silencing of endogenous ABCG2 does not affect the tumorigenesis of OCUM-2MLN cells

Next we examined whether the ABCG2 expression is functionally linked to the tumorigenic activity of OCUM-2MLN cells. We established the cells termed 2MLN-shRNA/ABCG2, whose expression of ABCG2 was stably knocked down by the transfer of short hairpin RNA (Supplementary Figure S1A). Though successful silencing of endogenous ABCG2 expression was achieved, 2MLN-shRNA/ABCG2 cells exhibited a

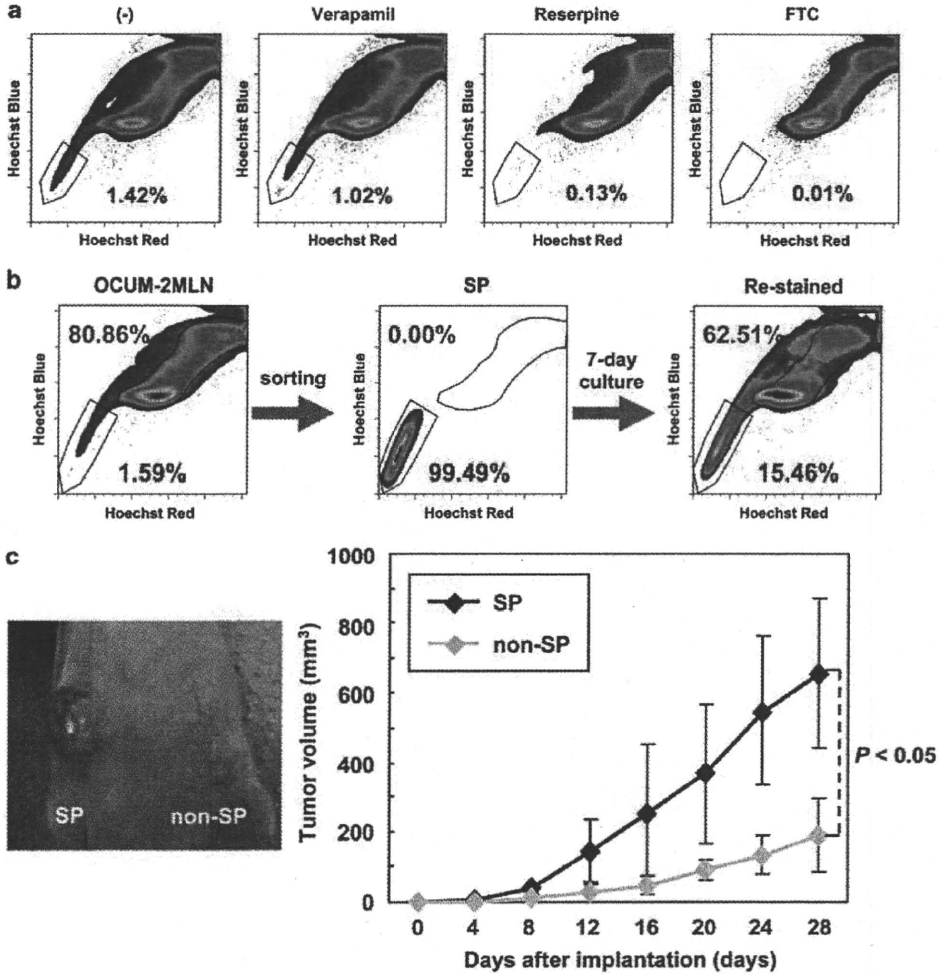

Figure 5 SP cells display tumorigenicity. (**a**) OCUM-2MLN cells were stained with Hoechst 33342 in the absence or presence of verapamil, reserpine or fumitremorgin C (FTC), and analyzed by flow cytometry. *Red numbers*, SP percentage of entire viable cell population. (**b**) SP cells were sorted from OCUM-2MLN cells. After 7-day *in vitro* culture of the separated cells, cells were re-stained with Hoechst 33342 and analyzed by flow cytometry. *Red numbers*, SP percentage of entire viable cell population; *Blue numbers*, non-SP percentage of entire viable cell population. (**c**) SP cells and non-SP cells were sorted from OCUM-2MLN cells separately. A total of 5×10^4 SP or non-SP cells were xenografted into BALB/c *nu/nu* mice. Representative photographs (*left panel*) and tumor volumes (*right panel*) were indicated. *Points*, mean; *bars*, s.d.

similar tumor forming ability to control 2MLN-shRNA/NTC cells *in vivo* (Supplementary Figure S1B). Thus, the importance of ABCG2 expression in cancer cells was not demonstrated by 'loss-of-function analysis', although this finding is consistent with previous reports, showing that $ABCG2^+$ and $ABCG2^-$ cancer cells exhibited similar tumorigenic abilities (Patrawala *et al*., 2005).

Cancer cells from metastatic sites include more SP cells than those from primary sites

Finally, we addressed the importance of SP cells in progression of diffuse-type gastric carcinoma using a series of gastric carcinoma cell variants from the same patient (Yashiro *et al*., 1994, 1996; Inoue *et al*., 1997; Fujihara *et al*., 1998): OCUM-2M (primary tumor), OCUM-2MLN (lymph node metastasis of orthotopically implanted OCUM-2M cells), OCUM-2MD3 (peritoneal metastasis of orthotopically implanted OCUM-2M cells) and OCUM-2D (pleural effusion of the same patient as yielded OCUM-2M cells) (Figure 7a). Flow cytometric analysis revealed that OCUM-2M, OCUM-2MLN, OCUM-2MD3 and OCUM-2D cells included SP cells at 0.00, 1.54, 0.14, and 0.04% of total cell populations, respectively (Figure 7b). Consistent with these findings, expression of ABCG2 in OCUM-2MLN cells was significantly higher than that in the other types of gastric carcinoma cells, and that TGF-β suppressed the expression of *ABCG2* messenger RNA (Figure 7c). In a mouse xenograft experiment, only OCUM-2MLN cells, and